STUDIES ON URBAN HEAT ISLANDS USING ENVISAT AATSR DATA

T.R. Kiran Chand, K. Madhavi Latha, K.V.S. Badarinath

National Remote Sensing Agency (Dept. of Space-Govt. of India), Balanagar, Hyderabad- 500 037, India
badrinath_kvs@nrsa,gov.in

KEYWORDS: Satellite Data, Surface Albedo, Surface Energy Balance, Evapotranspiration, Thermal Inertia, Urban Heat Island, Surface Temperature.

ABSTRACT:

In the studies related to surface energy balance, satellite data provides important inputs for estimating regional surface albedo and evapotranspiration. The paper describes the analysis of day and night AATSR satellite data for studying the urban heat island and surface thermal inertia. Field campaigns have been conducted in synchronous with the satellite data over pass for validating the surface temperature estimated from aatsr data. Satellite derived surface temperature values are within $\pm 1^0$ C from ground measured values. Heat island formations in urban regions of Hyderabad and environs can be clearly seen in the night time data with urban regions showing high temperatures. Apparent thermal inertia derived from AATSR day and night data sets showed typical variations over urban regions.

1. INTRODUCTION

The Urban Heat Islands (UHI) develop over cities as a result of anthropogenic activity, diverse surface cover and it represent the quality of climate over city. Besides, study of UHI help to understand the air quality, energy use, water use efficiency and human comfort. In cities, buildings and paved surfaces replace the existing green cover. As a result, solar energy is absorbed by the roads and rooftops, causing the surface temperature of urban structures to increase. Albedo is the measure of the amount of solar energy reflected by the surface. Low albedo imply higher surface temperatures and ambient air temperature due to higher absorption of incident solar energy. This phenomenon is known as an "Urban Heat Island". Satellite based thermal imagery offer data to study urban heat islands helps in studies related to regarding energy and water conservation, human health and comfort, air pollution dispersion and total air circulation. The cause for occurrence of urban heat islands is due to removal of vegetation cover and paving of the land surface by non-evaporating and non-porous materials such as asphalt and concrete(Lo and Quttrochi., 2003). The present study addresses the surface temperature estimation using AATSR data over urban regions for analyzing heat island formations. Advanced Along Track Scanning Radiometer (AATSR) is an advanced version of the ATSR system on board ERS-1 & 2. AATSR is a passive imaging instrument at 1 km resolution able to collect reflected and emitted electromagnetic radiation in 7 different spectral regions, spanning from the visible to the thermal infrared. The AATSR conical scanning mechanism allows the same area to be imaged twice at different viewing angles (nadir and 47 degrees forward) thus giving the possibility to estimate and correct for atmospheric effects and to improve the retrieval of Earth surface parameters (AATSR User Guide). NDVI estimated from AATSR has been taken as a parameter for estimating surface emissivity and algorithm based on nadir and forward scans of brightness temperature in 12μm has been used for estimating surface temperature.

2. DATA SETS AND METHODOLOGY

AATSR operates in channels with band centers at 0.555, 0.659, 0.858,1.61,3.70,10.85 and 12um. NDVI estimated from AATSR has been taken as a parameter for estimating surface emissivity and algorithm based on nadir and forward scans of brightness temperature in 12μm has been used for estimating surface temperature. ENVISAT AATSR data of 6th and 7th March, 2003 has been used in the present study. The present study explores the conceptual and methodological issues of taking NDVI of pure vegetation and bare pixels obtained form the reflectance's in NIR and red channels and using the information for the calculation of vegetation cover. The percentage cover has been used for estimating emissivity at pixel level.

NDVI is defined as

$$NDVI = (\rho_2 - \rho_1)/(\rho_2 + \rho_1) \quad \text{----------(1)}$$

where, ρ_1, ρ_2 are the reflectance measured in red and NIR wavelength bands respectively.

Considering a mixed pixel with a vegetation over P_v and a soil proportion $(1-P_v)$, the NDVI value (i) as a first approximation is

$$i = i_v P_v + i_g (1 - P_v) \quad \text{----------(2)}$$

where i_v and i_g are the vegetation and ground NDVI values respectively.

The vegetation fraction can be obtained from the NDVI by inverting equation (2). But this relationship is not correct (Price, 1990) because NDVI is a ratio and does not satisfy the associative property. This means that it is not the same, to weigh the reflectances in each channel and then calculate the NDVI, as the inverse procedure (applied to obtain equation (2)).

A mixed pixel reflectance is

$$\rho_n = \rho_{nv} P_v + \rho_{ng} (1-P_v) \quad \text{----------(3)}$$

where n = 1 for red and n=2 for near IR.

Substituting equation(3) in to equation (1), the NDVI becomes

$$i = \frac{P_v(\rho_{2v} - \rho_{1v}) + (1 - P_v)(\rho_{2g} - \rho_{1g})}{\text{----------}} \quad \text{----------(4)}$$

$$P_v(\rho_{2v} + \rho_{1v}) + (1 - P_v)(\rho_{2g} + \rho_{1g})$$

where ρ_{2v}, ρ_{1v} are reflectances in NIR and red region for pure vegetation pixels. ρ_{2g}, ρ_{1g} are reflectances in NIR and red region for pure soil pixels.

Equations (2) and (4) are not equivalent (Price, 1990). Depending on the reflectance values of each surface, the correction to equation (2) will be different. Thus a better way to relate the NDVI to the vegetation cover is,

$$i = i_v P_v + i_g (1 - P_v) + di \quad \text{----------(5)}$$

where di is correcting factor obtained by subtracting equation(2) from equation(4).

The proportion of vegetation cover is calculated using the relation (Valor & Caselles, 1996),

$$P_v = (1 - i/i_g) / [(1 - i/i_g) - k(1 - i/i_v)] \quad \text{----------(6)}$$

where, $k = (\rho_{2v} - \rho_{1v}) / (\rho_{2g} - \rho_{1g})$

Finally, the relationship between emissivity (ε) and NDVI of a given surface is,

$$\varepsilon = a\,i + b \quad \text{----------(7)}$$

where, $a = (\varepsilon_v - \varepsilon_g)/(i_v - i_g)$ and $b = [\varepsilon_g(i_v + di) - \varepsilon_v(i_g + di)]/(i_v - i_g) + d\varepsilon$.

For a given area the coefficient 'a' is constant, while coefficient 'b', changes from pixel to pixel with the type of vegetation cover and surface structure. General behavior of the shape of curve corresponding to the relationship between emissivity and NDVI is quite similar to the combination of a straight line and a quadratic expression. In order to define the error in emissivity (dε) values per pixel, a quadratic form has to be used. The dε takes value zero for $P_v = 0$ and $P_v = 1$.

$$d\varepsilon = 4 < d\varepsilon > P_v (1 - P_v) \quad \text{----------(8)}$$

where $<d\varepsilon>$ is mean weighted value taking into account the different vegetation in the area, their structures and their proportions in it. The maximum value of dε is given by $<d\varepsilon>$ and with a separation between boxes varying with P_v.
The following algorithm has been used for deriving surface temperature using AATSR data.

$$T_s = T_n + A*(T_n - T_f) + (1 - \varepsilon)*B_1 - \Delta\varepsilon * B_2$$

where A, B_0, B_1, B_2 are the double-angle coefficients. Based on the measured values of water vapor which are in the range 0.9 to 1.1g/cm^2, the values of coefficients have been taken as A = 1; $B_1 = 40$; $B_2 = 40$ (Sobrino et al., 1996); T_n and T_f are nadir and forward brightness temperatures at 12 μm. Portable meteorological kit has been used for measuring wind speed, wind direction, relative humidity and air temperature. Soil temperature probe has been used to measure soil temperature at 5 cm depth. Telatemp Model AG-42 IR thermometer has been used for estimating crop and soil surface temperature in field in synchronous with ENVISAT satellite pass. The instrument operates in the wavelength range 8 – 14 μm with an accuracy of $\pm$ 0.5°C and resolution of $\pm$ 0.1°C.

Thermal inertia, TI, is a physical property of materials describing their impedance to temperature change. The equation $TI = (K\rho c)^{1/2}$, shows its dependence on the thermal conductivity K, density ρ and specific heat c of the material. The change in temperature at the Earth's surface due to a given heat flux is inversely related to the thermal inertia of the exposed material. In particular, water bodies, having TI higher than dry soils and rocks, exhibit lower diurnal temperature fluctuations. As soil water content increases, thermal inertia also increases, reducing the diurnal temperature range. Present satellite remote sensing capabilities in measuring Earth surface temperature can be exploited in order to derive information on soil moisture, provided that the re-visitation time is adequate to follow the diurnal temperature cycle and the spectral resolution is sufficient to evaluate the net heat flux at the Earth surface. An approximate (Apparent) value (ATI) of the actual TI, can be obtained from ENVISAT AATSR measurements of the spectral surface albedo A and of the diurnal temperature range DT, as ATI = (1 – A)/DT. Surface albedo A was obtained using visible and near-infrared reflectances from AATSR channels. The diurnal temperature range DT is the difference between surface temperatures, T, measured in the AATSR thermal infrared channel at noon and midnight DT = (T5day- T5night). Actual values of TI and measured ATI are variously affected by parameters related to space–time variability of observational, atmospheric, and surface conditions (e.g. time of the pass, satellite/solar zenith angles, transmittance, cloud cover, vegetation).

3. RESULTS AND DISCUSSION

Fig. 2a shows the AATSR bands 0.87μm, 0.67μm and 0.55 μm FCC of study area. Field experiments on surface temperature estimation have been conducted in paddy crop areas located at center of the image. The determination of surface temperature from satellite data requires the knowledge of emissivity of various land surface features at the sensor resolution. In the present methodology, the determination of surface emissivity requires the use of satellite data together with some emissivity values of vegetation types from literature. Since, we do not have prior information on emissivity values of the area, the mean emissivity value of 0.88 for bare soil and 0.986 for vegetation in 8-14μm region has been taken (Carnahan and Larson, 1990). The emissivity values over soil have been confirmed with the field measurements on measured soil temperature and radiant temperature. In order to estimate the term $<d\varepsilon>$, three main vegetation structures have been considered and mean value of emissivity in 8-14 μm region has been taken. The mean value of $<d\varepsilon>$ has been taken as 0.01. Calculation of proportion of vegetation cover needs reflectance of pure pixels of vegetation and bare soils in NIR and Red channels and these values have been taken from the AATSR data gridded (AATSR product type ATS_TOA_1C) provided by ESA. The maximum NDVI value in the present data set is 0.65 and minimum of 0.11. The proportion of vegetation cover has been calculated using equation (6). Percentage vegetation cover (P_v) image generated from AATSR is shown in Fig. 2(b) and the values of P_v vary depending on the proportion of vegetation in the 1km resolution pixel. Surface emissivity per pixel has been estimated using equation (7). Emissivity image generated from AATSR is shown in Fig. 2(c). The emissivity

values derived from the present methodology have been compared with values in 8-14μm range over some known features (Valor and Caselles, 1996) and are found to be in reasonable agreement with an error not exceeding 1%. Surface temperature estimated using day and night time data of AATSR is shown in Fig. 2(d&e) and the comparison of field measured surface temperature with satellite data suggested variation of $\pm$ 1^{o}K. The values of surface temperature estimated using AATSR has been found to be in acceptable range over the study area. The surface temperature is minimum over water surface (18-21^{0}C) and maximum over urban areas (36-40^{0}C). Apparent thermal inertia image generated from day and night surface temperature data of AATSR has been shown in Fig. 2f.Apparent thermal inertia derived from AATSR showed typical variations matching with urban land use variations viz., dense, medium and sparse urban areas. The information on urban heat island formation and its spatial variation provides planners to incorporate mitigation measures such as avenue plantations, recreation parks with vegetation cover etc. Further studies have been planned for validating methodology adapted in the present study.

Figure1: Location map of the study area

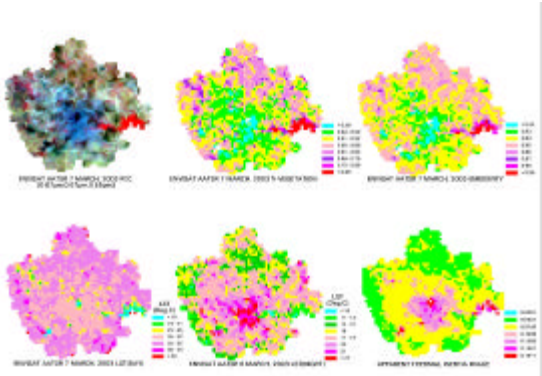

Figure2:
(a)FCC of visible and near-IR bands of AATSR
(b) Percentage vegetation map (c)Emissivity image
(d) Land surface temperature image during daytime
(e)Land surface temperature image during nighttime
(f) Thermal inertia image

4. CONCLUSIONS

The analysis of ENVISAT-AATSR data over urban regions of Hyderabad suggests that

(1) AATSR day and night data can be used for monitoring nature and extent of urban heat islands
(2) Apparent thermal inertia derived from day and night datasets provides information on thermal storage spatially over urban areas.
(3) The information derived from AATSR can be used for urban planning activities in terms of avenue plantations and recreational parks for reducing heat island formations.

REFERENCES

Caselles,V., Sobrino,J.A and Coll,C., 1992. On the use of satellite data for determining evapotranspiration in partially vegetated areas. Int. J. Remote Sensing, 13: 2661-2682.

Kustas,W.P., Jackson and Asrar., 1989. Estimating surface energy-balance components from Remotely sensed data. Chapter 16- Theory and Applications of Optical Remote Sensing. A Wiley-interscience Publication.

Lo, C.P.,and Quattrochi, D.L., 2003. Land-use and Land-cover change, urban heat island phenomenon and health implications: A Remote Sensing Approach. Photogrammetric Engineering & Remote Sensing, 69(9),1053-1063.

Batiaanssen, W.G.M., Menenti. M., Feddes, R.A., Holtslag, A.A.M., 1998. A remote sensing surface energy balance algorithm for land(SEBAL), Journal of Hydrology, 212-213: 198-212.

Goita,K and Royer, A., 1997. Surface temperature and emissivity separability over land surface from combined TIR & SWIR AVHRR data. IEEE Trans.on Geoscience & Remote Sensing, 35: 718-733.

Carnahan,W.H and Larson,R.C., 1990. An analysis of an urban heat sink. Remote Sensing of Env.,33: 65-71.

Valor., E and Caselles,V. , 1996. Mapping Land surface emissivity from NDVI : Application to European, African & South American Areas. Jl of Remote Sensing of Env., 57:167-184.

Price, J.C., 1990. Using spatial context in satellite data to infer regional scale evapotranspiration. IEEE trans. Geoscience and Remote Sensing, 28: 940-948.

Sobrino, J.A., Li, Z.L., Stoll, P. and Becker, F., 1996. Multi-channel and multi-angle algorithms for estimating sea and land surface temperature with ATSR data. Int. Jl. Of Remote Sensing, 17: 2089-2114.

Valor., E and Caselles, V. , 1996. Mapping Land surface emissivity from NDVI : Application to European, African & South American Areas. Jl of Remote Sensing of Env., 57:167-184.

ACKNOWLEDGEMENTS

Authors are grateful to Director, NRSA and Dy. Director (RS&GIS-AA), NRSA for their help and encouragement and ISRO-GBP for funding support.